Nano Energy 78 (2020) 105216

Contents lists available at ScienceDirect

Nano Energy

journal homepage: http://www.elsevier.com/locate/nanoen

A triboelectric-piezoresistive hybrid sensor for precisely distinguishing transient processes in mechanical stimuli

Zhihao Ma [a,1], Bo Meng [a,1], Ziya Wang [a], Chaocheng Yuan [a], Zhangwei Liu [a], Weiguan Zhang [b], Zhengchun Peng [a,*]

[a] Key Laboratory of Optoelectronic Devices and Systems of Ministry of Education and Guangdong Province, College of Physics and Optoelectronic Engineering, Shenzhen University, Shenzhen, 518060, China

[b] Key Laboratory of Micro/Nano Optomechatronic Engineering of Guangdong Province, College of Mechatronics and Control Engineering, Shenzhen University, Shenzhen, 518060, China

ARTICLE INFO

Keywords:
Tactile sensor
Triboelectric nanogenerator
Active sensing
Piezoresistive sensor
Hybrid sensing
Transient mechanical stimuli

ABSTRACT

As a pivotal component in human-machine interface and autonomous robot, tactile sensors are imperative to own extra capability of perceiving transient mechanical stimuli, rather than remaining in the static sensing regime. In this work, a hybrid tactile sensor is proposed, which integrates a porous polydimethylsiloxane (PDMS) based triboelectric active sensing unit and a conductive carbon black (CB)/thermoplastic polyurethane (TPU) composite based piezoresistive sensing unit. This hybrid sensor responds well to both static and transient mechanical excitations, such that the entire process of "approach-contact-press-release-separation" in a tactile stimulus can be precisely distinguished. In addition, this sensor can detect the approaching and separating speed up to 100 mm s^{-1}, with a good linearity between the contact or separation speed and the triboelectric voltage output. The two signals from the hybrid sensor can be combined to generate comprehensive and insightful information about a mechanical stimulus and differentiate nuances among similar stimuli. We demonstrate the application of the hybrid sensor in a smart boxing-training glove, which is capable of identifying different boxing punches and revealing detailed information about the impact of each punch.

1. Introduction

The rocketing development of artificial intelligence necessitates a great number of sensors, including auditory, visual and tactile sensors, for comprehensive information acquisition. Tactile sensor, which measures information from physical interaction by converting mechanical stimuli into electrical signals, has played an essential role in the modern consumer electronics industry. Moreover, it is a pivotal component of wearable electronics for health monitoring and motion-detecting, as well as of electronic skin for smart robotic operation [1,2] and human-machine interface [3–7].

In addition to improving the performance of the mainstream tactile sensors such as piezoresistive [8–10], capacitive [11,12], and piezoelectric sensors [13,14], researchers have also sought for active sensing, which means sensors that can detect the stimuli without an external power source, in recent years [15]. Triboelectric nanogenerator (TENG) has undergone a long period of development in basic theory and is gradually being improved [16–21]. Even though there are still some puzzles [22], the available theories provide sufficient instructive guidance for designing the structure and optimizing the properties in both energy harvesting and active sensing [23–39]. What's more, with the exploration of flexible materials in TENG deisgn, TENG has strode forward to the flexible electronics field [34]. The conversion of ambient mechanical vibration to electric energy could take place in extensive scenarios. These electrical outputs can be employed for sensing purposes as well, making TENG a competitive active sensing solution. In addition, combinations of structure design and material selection open up a wide range of possibilities for TENG active sensor in many specific applications. As such, TENG was used in auditory sense system [35], trajectory detection [36], bending detection [37], even the detection of mercury ions [38], and gas [39]. In the segment of the tactile sensor, the mechanism of contact electrification has advantages in high sensitivity and responding to dynamic stimuli [40–43], and has been employed in robotic tactile sensing, touchpad, and pressure mapping [44–47].

* Corresponding author.
E-mail address: zcpeng@szu.edu.cn (Z. Peng).
[1] These authors contributed equally to this work.

https://doi.org/10.1016/j.nanoen.2020.105216
Received 20 June 2020; Received in revised form 16 July 2020; Accepted 22 July 2020
Available online 15 August 2020

The mono-functional sensors can hardly satisfy the demand for the acquisition of complex information. Hence, there is big demand for hybrid sensors that detect multidimensional information from one mechanical stimulus. TENG has expanded the option of making hybrid system [48–51]. For example, the combination of TENG and supercapacitor makes a self-powering sensing system that could work without external power supply [48]. Because of the high sensitivity to pressure, TENG is also combined with a mechanoluminescent sensor in a pressure sensing system, in which TENG is used for detecting pressure in the low range and the mechanoluminescent counterpart in a higher range [49]. A paradigm of the hybrid tactile sensor is inspired by human fingerprint. For instance, one can combine a slide sensor and a press sensor to distinguish different texture of an object by simultaneously obtaining their sliding and pressing characteristics [50].

Admittedly, works mentioned above have realized the acquisition of multidimensional information in various stimuli. However, these hybrid sensors gather independent information without considering the concerted effect among different sensing mechanisms. Aiming at unifying independent signals into one comprehensive signal for identifying complex mechanical stimuli during a contact-and-separation process, we propose a tactile sensing strategy from not only the pressure perspective, but also the approaching process before impending the contact.

Herein, we present a hybrid tactile sensor based on the combination of triboelectrification and piezoresistive effects. A TENG active sensor and a piezoresistive pressure sensor are integrated horizontally to guarantee that stimuli can generate signals on two tactile units concurrently. The TENG is sensitive to the approaching and separation processes, while the piezoresistive sensor responds well to the pressure when contact occurs. Using the bi-signal generated from this hybrid sensor, one can precisely analyze a complex mechanical stimulus. The combination of the active sensing with the passive sensing enables the hybrid sensor to distinguish mechanical stimuli that apply identical pressure but with minutely different processes.

2. Results and discussions

2.1. Design and process of the hybrid sensor

The schematic of the hybrid sensor is outlined in Fig. 1a. Structurally, the hybrid sensor consists of two parts. A single electrode TENG composed of porous PDMS friction layer and Cu electrode is employed for tactile detection. When an object approaches and contacts the sensor, the charge would transfer between the surfaces since the materials possess the different ability to gain or lose electrons. The alternating voltage generates while the contact-separation process occurs on the device between the triboelectric electrode and the grounded electrode. Fig. S1 (supporting information) shows the detailed working mechanism of the single electrode TENG. The triboelectric active sensing mechanism has an advantage in capturing motion information. Meanwhile, the piezoresistive sensing unit composed of porous conductive CB/TPU sponge and interdigitated electrodes serves as pressure detector based on the variation of contact resistance under compression. The coplanar design guarantees that one mechanical stimulus converts into triboelectric signal and piezoresistive signal concurrently. Hence, these two signals complement each other to form a bi-signal judgment which apprehends one contact process not only from the contact effect but also the approaching process. The single electrode TENG is responsive to the motion of contact and separation process, and the piezoresistive part is sensitive to the load and the duration time on pressure.

Fig. 1. b schematically illustrates the fabrication process of the hybrid sensor. The manufacture starts from a polyimide (PI) substrate

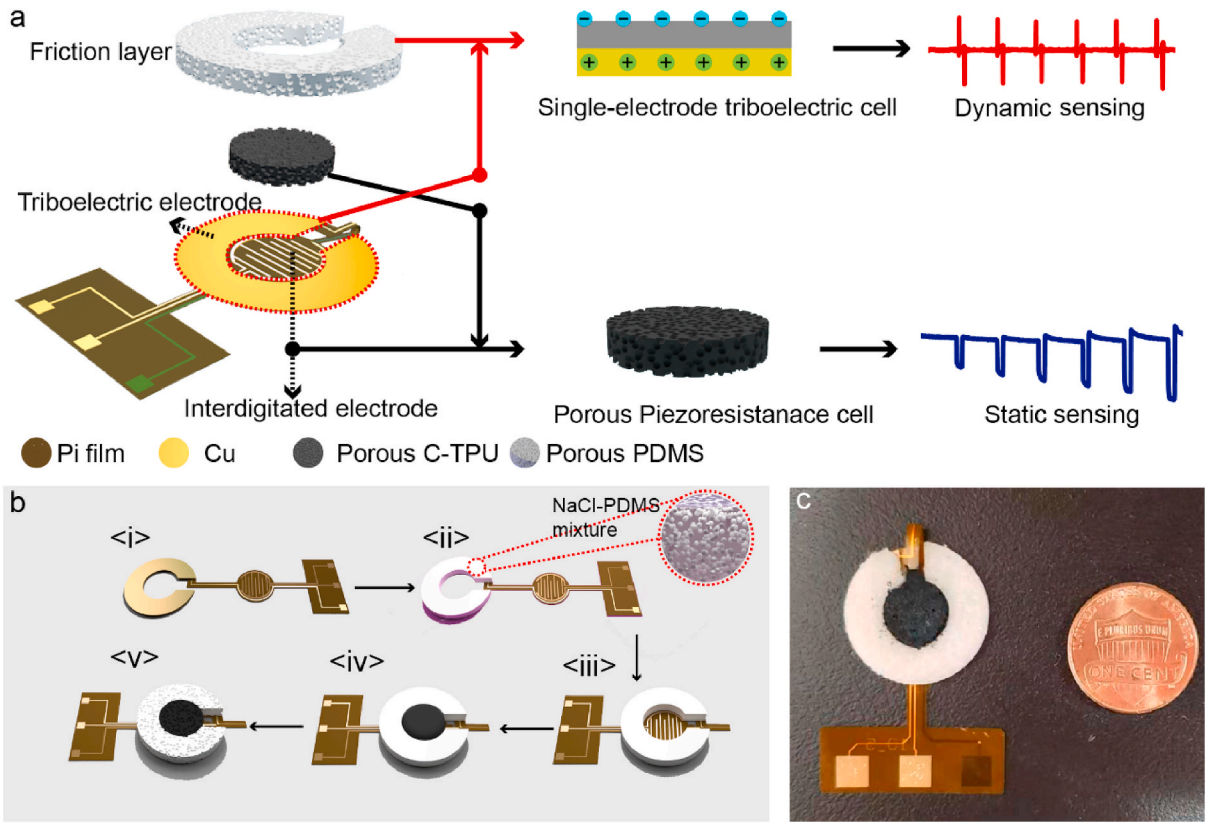

Fig. 1. Design principle of the hybrid sensor and the scheme of the process. a) The Schematic of the hybrid sensor with the TENG sensing the dynamic mechanical stimuli, and the piezoresistance cell sensing static stimuli. b). The fabrication process of the hybrid sensor with the two sensing parts being integrated laterally. c) Photograph of the as-fabricated hybrid sensor.

with gold coated copper electrodes on the surfaces (Fig. 1b<i>). The ring-shaped triboelectric electrode was embedded into a 2 mm thick acrylic template, then the mixture of PDMS and NaCl particles was cast into the template. After curing at 80 °C for 1 h (Fig. 1b<ii>), the solidified mixture is lifted out. Then, the substrate was folded with aligning the centers of annular and circular electrodes to be concentric homocentric. This state (Fig. 1b<iii>) serves as the template for a molding mixture of CB/TPU/NaCl. The CB/TPU/NaCl mixture was filled in the template which folded from the substrate with cured PDMS on it. After molding, the sensor was cured and dried at 80 °C in a vacuum oven for 24 h. Once the curing process finished (Fig. 1b<iv>), the NaCl particles were dissolved by immersing the sensor in 60 °C deionized water for 24h. After the evaporation of residual moisture, the hybrid sensor is fabricated (Fig. 1b<v>). The CB/TPU/NaCl mixture is cast after the PDMS mixture is cured, by following this manufacturing sequence, it can guarantee the insulation between the electrodes by prevent the mixture from oozing to the triboelectric electrode. The as-fabricated coin-sized hybrid sensor is shown in Fig. 1c. The overall height of the device is 2 mm, the radiuses of the united device and piezoresistive part are 10 mm and 5 mm, respectively.

The material selection strategy finalizes from two aspects: stable performance for individual unit and the appropriate modulus matching. Because of its weak performance (0.4 V) in triboelectric voltage outputs when paired with copper (Fig. 2a). We eliminate the triboelectric candidate material (porous TPU elastomer). For the piezoresistive unit, we chose NaCl particles of 300–355 μm diameter as the sacrificial template to form the porous structure, as this pore size is more sensitive than other size we tested to the pressure range we are interested in (Fig. 2b and Table S1 in supporting information). The pressure curves were measured under cyclic loading with 79.6 kPa applied through square wave vibration motion type. For modulus matching, we control the friction layer of TENG to be softer than the piezoresistance elastomer to prevent that friction layer is dominant during the deformation process which will counteract the load exerted on the piezoresistive unit. The NaCl particles mixed in PDMS are also in size of 300–355 μm because the NaCl particles in this size interconnect well in the mixture so as to be dissolved into the water more efficiently. Fig. 2c shows the SEM image of porous PDMS, and Fig. 2d, **e**, **2f** shows the SEM images of porous conductive C-TPU elastomer with varying diameters of the pore. After determining the above conditions, we control the softness of PDMS by adjusting the curing agent ratio. Admittedly, the horizontal integration method lowers the sensitivity of the load detection, compared with the individual piezoresistive unit, as the comparison is shown in Fig. S2 (Supporting information). Nevertheless, this structure extends the detection range and becomes insensitive to small forces and reduces signal jitter caused by damped vibration when the stimulus applicator contacts the sensor. For triboelectric sensing, the integration keeps insulation between the triboelectric electrode and piezoresistive elastomer, avoids the interference between two paths. Therefore, two sensing parts of hybrid sensor can both work independently without mutual influence.

2.2. Characteristic of the hybrid sensor

Elaborated design of fabrication and proper selection of material ensure that the hybrid sensor well responds to two types of signals. On the static sensing part, the piezoresistive sensing unit reaches a sensitivity of 2.1 MPa^{-1} in a range of below 70 kPa (calculated with the whole size of the hybrid sensor), as the piezoresistive curve of the sensor is shown in Fig. 3a. And, the maximum force that can be detected is 120 N (or 384 kPa). The average response time and releasing time are 46 ms and 41 ms, respectively, measured by different load tests, as its shown in Fig. S4 (Supporting information). On the TENG active sensing part, the output voltage and short-circuit current of the TENG are shown in Fig. 3b and c, respectively. When a 1 Hz frequency pressure test sequence exerts on the sensor, the peak value of output voltage and short-circuit current are stabilized at 13.4 V and 11.8 μA. Hence, the outputs are qualified for active sensing. Moreover, the TENG active sensing part improves the pressure sensing limitation to about 0.59 kPa as well. To prove that a hybrid sensor has resilience and robustness in the working situation, we set up a test procedure with five stimulus sections, the excitation frequency is from 1 Hz to 5 Hz, and each part lasts 200 s, the interval between mode changes is 2 s. The bi-channel signal generated by the fatigue testing program shows in Fig. 3d. The

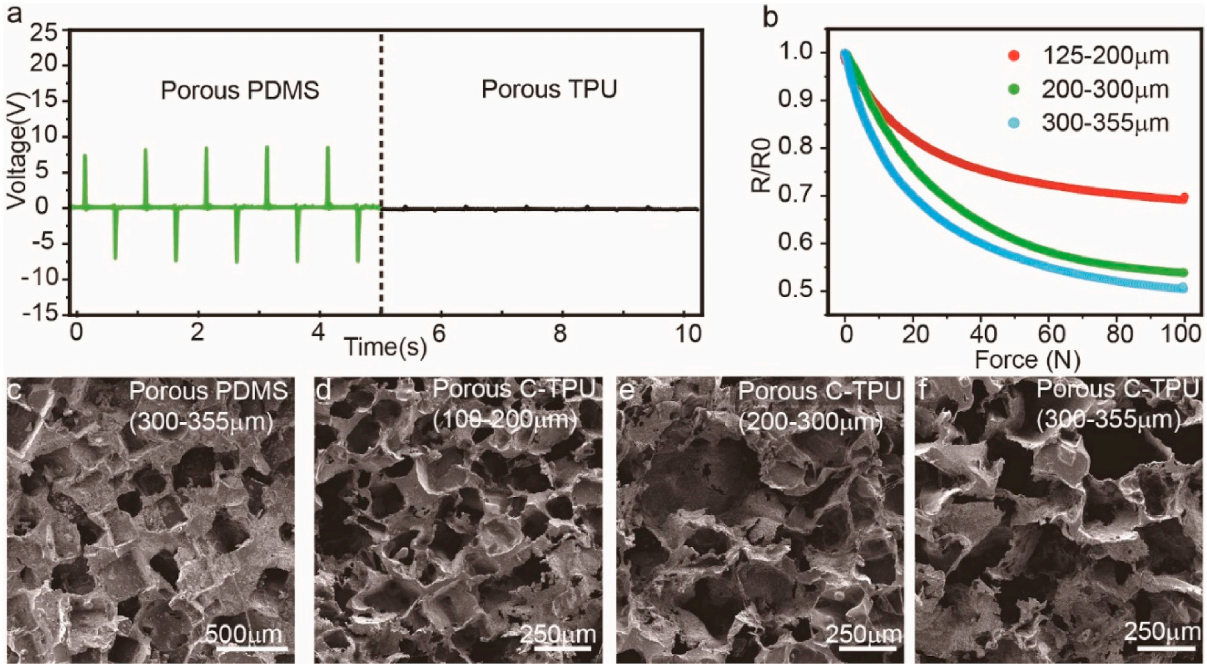

Fig. 2. Material selection of the hybrid sensor. a) The voltage output of porous PDMS and porous TPU for serving as friction layer under the same testing program. b) Pressure curve comparison of conductive porous C-TPU sponge with different pore diameters. c) SEM image of porous PDMS. d-f) SEM images of porous conductive C-TPU sponge with varying diameters of the pore.

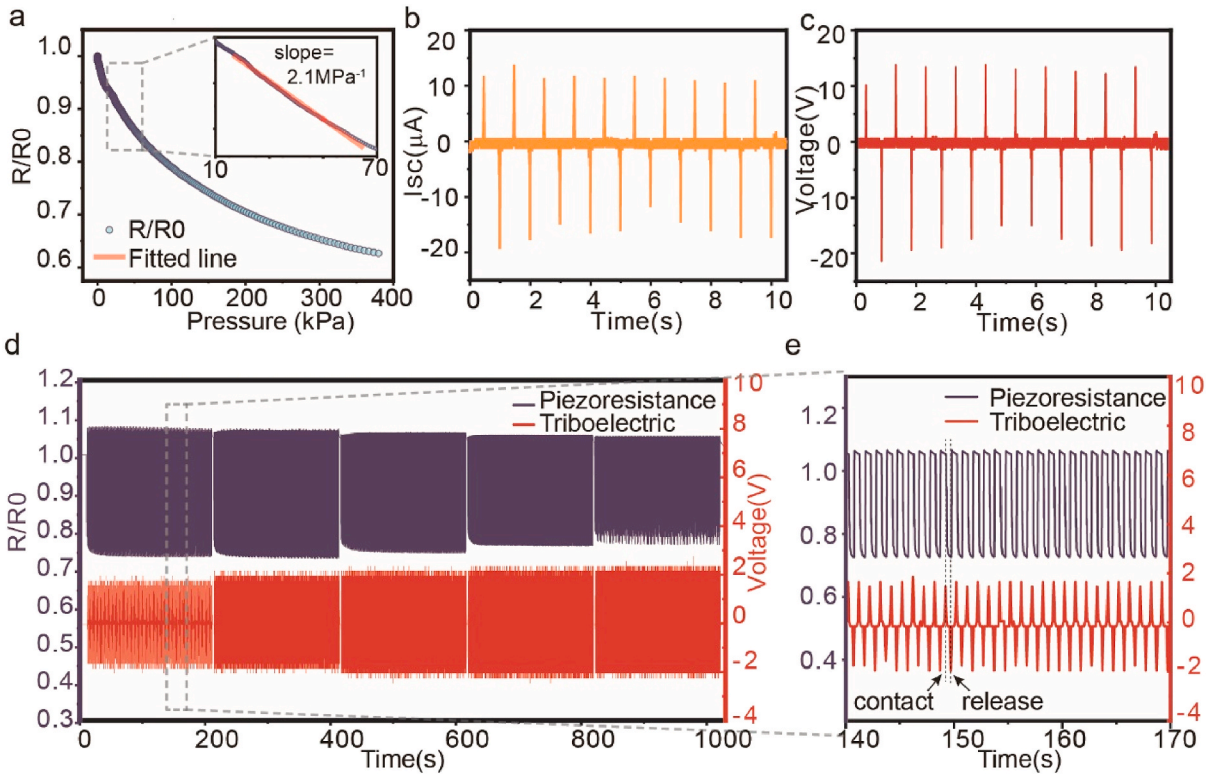

Fig. 3. Characterizations of hybrid tactile sensor. a) Pressure curve of the hybrid sensor. b) Short-circuit current output of the hybrid sensor on 1 Hz mechanical simulation. c) The Output voltage on 1 Hz mechanical simulation. d) Piezoresistive and triboelectric bi-channel output generated by fatigue testing program during 1000 s. e) The bi-channel signal during 30 s of the fatigue testing.

piezoresistive signal keeps stable in totally 3000 cycles within 1000 s. Notably, the amplitude of the voltage has a tiny rise following the frequency shift. Fig. 3e shows the synchronicity of two signals by zooming in the time scale of the signal from fatigue testing. Further, the device shows a good long-term stability over a test of 10,000 cycles at 1Hz (Fig. S5 in Supporting information).

Under the precondition that the hybrid sensor was tested as a single entity and obtain a stable signal, we also study on the relationship between the speed and triboelectric voltage output, and we combine it with piezoresistive signals into the bi-channel signal as a criterion for identifying the stimuli. To characterize the hybrid sensor, we use the mechanical testing system to supply the mechanical stimuli and a Wheatstone bridge to convert the resistance variation into a voltage signal, so that we can capture them by one oscilloscope simultaneously. The configuration of the testing environment is shown in Fig. S6 (Supporting information) and the schematic of converting circuit is shown in Fig. S7 (Supporting information). The influence of the parasitic capacitance caused by the piezoresistive unit on TENG's output is discussed in Fig. S8 (Supporting information), The noise signal from the parasitic capacitance is very tiny when the hybrid sensor is characterized under the schematic shown in Fig. S7. Because of the different sensing mechanisms, the electric signals triggering condition of triboelectric sensing and piezoresistive sensing differ in contact distance. We manipulate the contact distance between the press-head and original position of the sensor's top surface are ranging from 0.7 mm to −1.1 mm, and the negative value means the sensor is being compressed. As shown in Fig. 4a, the triboelectric signal is distinguishable under the contact distance of 0.7 mm, and it becomes clear and easy to catch when the contact distance drops to 0.4 mm. Meanwhile, the piezoresistive signal is indistinguishable from background noise under the contact distance of 0.2 mm, and it becomes distinct till contact distance goes to −0.2 mm. The result means under the non-contact range (0.1 mm–0.7 mm) TENG works to sensing the approaching process before contact. Once compression occurs, the piezoresistive unit starts to detect the pressure. Therefore, by correlating piezoresistive static sensing and the triboelectric dynamic sensing signal, the tactile detecting range extends to the non-touch area, which has great significance for the detecting approach motion of mechanical excitation. Piezoresistance takes more care about the contact situation, which only occurs after stimuli exerted, and it contains information of duration time and the load. Meantime, the TENG is more related to the approaching process, which implies how stimuli impose on the sensor. The amplitude of the triboelectric signal is primarily related to the contact-separation speed. We set the constant contact distance to −1.5 mm and the separate velocity to 100 mm s^{-1}, then exert the pressure with different contact speeds on the sensor. As the result shown in Fig. 4b, the voltage amplitude rises with increasing contact speed, especially in the range of 1 mm s^{-1} to 100 mm s^{-1}. Then we change the experiment setup into that the detach speed is variant and the contact speed is constant. As the result shown in Fig. 4c, the trends and the peaks of ascending signals produced by the contact operation in the whole contact-separation process keep steady in seven stimuli. On the contrary, the descending signal generated by the separation process increases following the boosting separation speed. What's more, the relationship between contact/separation speed and voltage output amplitude appears linear in the range of 1–100 mm s^{-1} and 1–50 mm s^{-1}, respectively (Fig. 4d). Meanwhile, a linear range of 1–160 mm s^{-1} is observed between contact speed and the short-circuit current amplitude of the TENG (Fig. S9 in supporting information). The mechanisms of this linearity is discussed in Fig. S10 (supporting information). Then, we change the testing program of this instrument, set the contact force as a variant, and keep the speed of contact and separation to a fixed value. When the force increases from 1 N to 55 N, the piezoresistive signal is sensitive to the pressure. But the amplitude value of the triboelectric signals under different excitations are distributed in the scope of 3.66V–4.02V. It is corroboration that the triboelectric output is much more sensitive to the contact-separation speed than force, even though

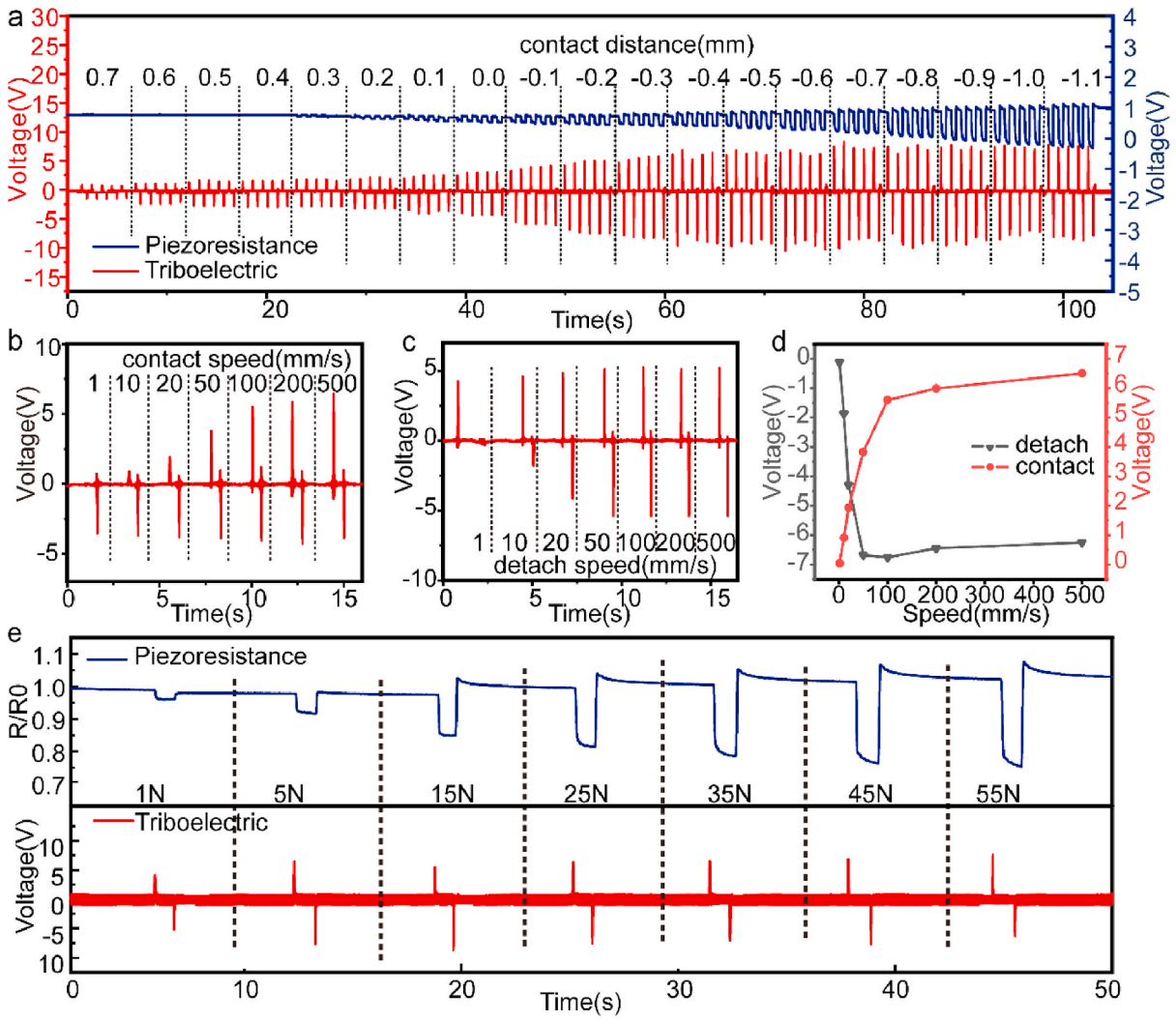

Fig. 4. Detection range and speed sensitivity of the hybrid sensor. a) The detection range of piezoresistive sensing unit and TENG in contact distance perspective. b) The voltage output generated from the contact speed testing sequence. c) Voltage output generated from mechanical stimuli that contain different separation speeds. d) Linearity relationship between contact/detach speed and the TENG's voltage output. e) Bi-channel outputs under the stimulation sequence. This sequence contains seven steps, and each step shares identical contact-separation speed but differs in load.

the triboelectric signal contains the information of speed and force, as to our hybrid sensor. The triboelectric tactile sensor excavates the information of dynamic mechanical changes and articulates it through triboelectric output. Therefore, such resultant bi-channel signals can not only perceive the contact force and duration time of pressure but also recognize the speed information of approaching and separating process. The triboelectric part fills the piezoresistance sensor's lack of detection range and insensitivity of speed information. Parallelly, the piezoresistive unit provides sensitive and reliable pressure detection. Triboelectric tactile and piezoresistive tactile sensing signal are mutually beneficial rather than superfluous to each other. The informative bi-signal judgment is a powerful tool when encountering the complicated situation which could hardly be discerned by a triboelectric tactile sensor or a single pressure sensor alone. It shows advantages in identifying complicated and multistage force process, in which the correlation between the proximity motion before contact and the pressure at which contact occurs is not one-to-one correspondence. Namely, the force under the same load could be applied by diverse patterns. But with the ability to gather information from two perspectives for more accurate identification, this hybrid sensor has suffered various kinds of mechanical stimuli and has survived in those complex situations successfully.

2.3. *Distinguishing transient processes in mechanical stimuli*

This hybrid sensor builds a bi-signal to distinguish different actions in life scenarios, piezoresistive unit and TENG are both indispensable. We exert two actions, "touch" and "press" on the hybrid sensor by a machine, and the definition of "touch" is that the pressure exerted must be within 1 N, the load for "press" is about 20 N. For "touch" action, in which the piezoresistive part hardly generates a valid signal because the pressure is slight. However, the triboelectric signal can indicate the contact and separation timing, as shown in Fig. 5a<i>. The triboelectric signal reflects when "touch" is exerted and released on the hybrid sensor, but if we only consider the triboelectric signal, we will not be able to identify whether the action is "touch" or "press" action. Once we add the pressure information into consideration, two actions are distinctive because they differ in pressure, the bi-channel signals of press action shows in Fig. 5a<ii>. And then we initiate the "tapping" and "knocking" by hand on hybrid sensor. Results are shown in Fig. 5a<iii> and Fig. 5a<iv>, continuous tapping and knocking that generated similar same voltage outputs, which can hardly be distinguished by the triboelectric path alone. But they are distinguished successfully by bi-signal judgment, since the pressure information is added into the judgment, the piezoresistive unit identifies the degree of pressure. Parallelly,

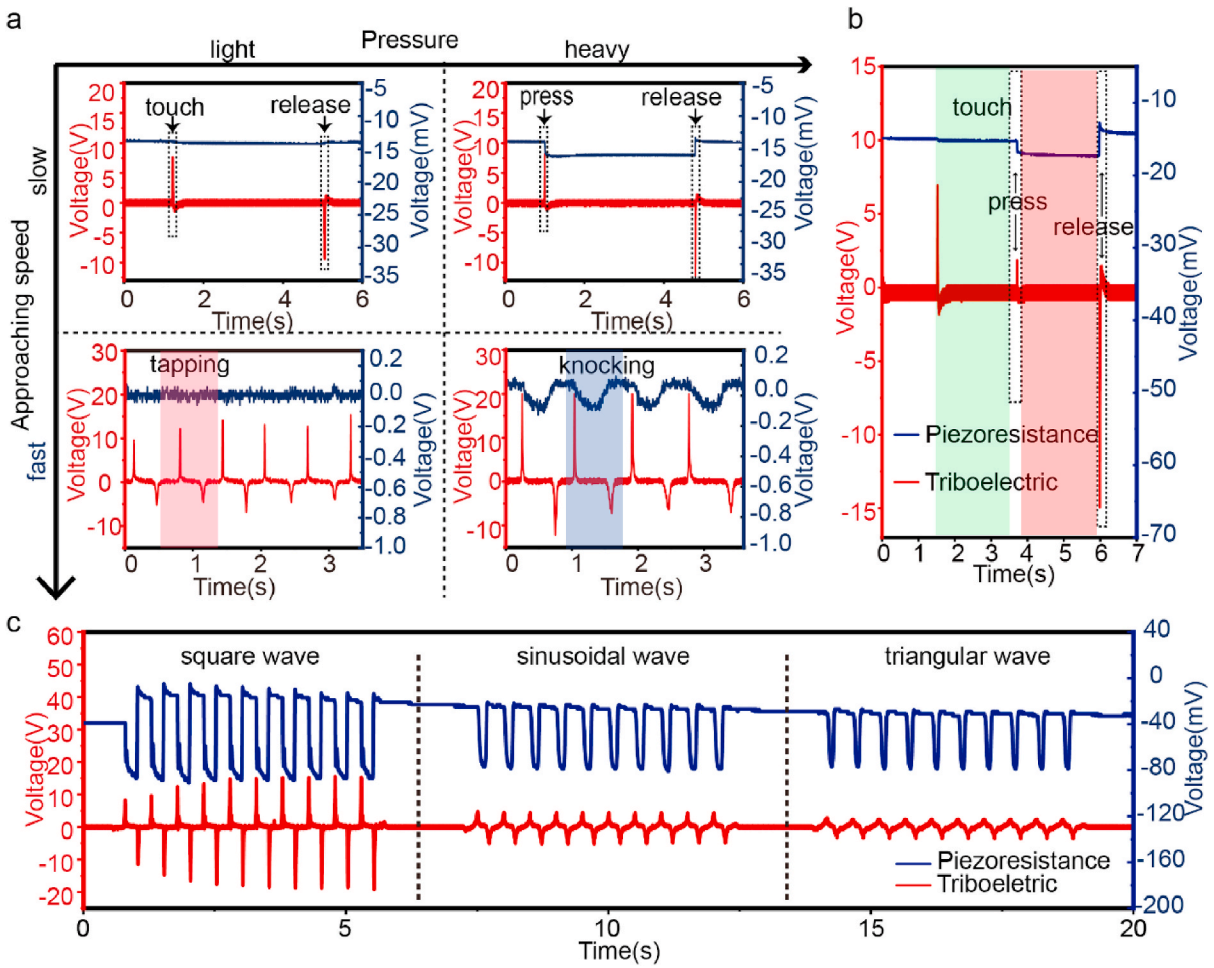

Fig. 5. Bi-signal criteria for distinguishing different mechanical stimuli. a) Bi-signal output generated from different actions that differ in pressure and approaching speed. b) Bi-signal outputs from a multistage action. c) Bi-signal output generated from three mechanical stimuli that are under the same force but applied via different motions.

when actions share the same pressure, we can distinguish them through the approaching information. For "tapping" and "touch" action, the pressure is imperceptible to our hybrid sensor. But according to the approaching speed information, the slower action (touch) generates lower triboelectric output. Tapping, the action possessing the faster contact speed generates higher triboelectric output. If bi-channel contains information that contact and separation speed is high and acting time is rapid, we will judge this stimulus with sudden pressure is "striking" action. Conversely, "squashing" which applies the same force compare with the strike action, defined as contacting slowly first and then pressing, cannot induce the higher voltage output, even if force more. The bi-channel signal of the "squashing" and "striking" applied by finger, are shown in Fig. S11 (Supporting information). The results above show that the piezoresistive signal can hardly distinguish the stimuli which have the same force but are applied in different ways, once the judgment of contact-separation speed information is missing.

Moreover, the actions in life scene are usually complicated and multistage, and we choose the "approach-contact-press-release-separation" as a study object, which includes slow touch and subsequent press. We program this process on the testing machine, the time-force, and time-displacement functional relationship are shown in Fig. S12 (Supporting information). By exerting this compound action on the hybrid sensor, the bi-channel signal will correctly recognize such motion, as shown in Fig. 5b, the "touch" with the specific contact speed (240 mm s^{-1}) rises the voltage amplitude, but the negligible pressure hardly generates the valid piezoresistive signal. When the "press" action with 28 N force exerts on, the pressure detection channel keeps on −16mV. Subsequently, the recovery of the piezoresistive signal and the rapidly descending triboelectric signal indicate that the action is complete. Also noteworthy is that the ascending triboelectric signal (1.98V) takes place at the action transition point, it marks the beginning of the "press" action. Meanwhile, it can reflect whether it forces slowly or rapidly.

In addition to distinguishing the actions in life, this hybrid sensor can also identify typical industrial mechanical excitations. We program three kinds of mechanical excitation which are the same in compression distance but different in approaching and detaching motion. The functional relationships between the distance of press-head to sensor and the time $z(t)$ of these three motion modes are similar to square wave, sinusoidal wave, and triangular wave, we label these three modes with SQU, SIN, and TRI, respectively. We set the same amplitude for these three vibration modes to ensure the lowest position ($z_{min} = -1.7$ mm) are identical. Therefore, the force applied in the three modes are equal. Then run the program to apply same pressure with different motion models on the sensor. The bi-channel signal is shown in Fig. 5c. The triboelectric output peak under SQU mode is highest because the contact-separation speed is faster than the other two, reach to 15 V. For SIN and TRI excitation modes, their differences of motion patterns reflected in piezoresistive path are so imperceptible that pressure sensing signals show little difference. However, we can distinguish these two excitation modes through triboelectric waveforms. The trend of the triboelectric signal generated by SIN mode climbs and drops more rapidly than the signal generated by TRI mode. The peaks of the

triboelectric signal generated by the SIN and the TRI mode are 4.2 V and 1.8 V, respectively. Plus, we use the full width at half maximum (FWHM) of the triboelectric output waveform as valid information for distinguishing SIN mode and TRI mode, which are different subtly. The FWHM of triboelectric output waveform under SIN mode and TRI mode are 0.20 s and 0.11 s, respectively. Regard to the 2 HZ excitation frequency, the width of the single whole waveform is about 0.5 s, FWHM is a rational judgment for these two nuanced excited modes. This result shows the approaching speed sensing mechanism provided by TENG is sensitive to nuance in motion mode, which cannot be detected by the piezoresistive signal.

2.4. Application in motion detection

The presented hybrid sensor has an advantage of sensing the motion process before contact, and it has great significance for practical applications in sports scenes. The strategy is to convert sports actions into an electrical signal, and then construct the criteria of actions. In addition, it provides feedback information to help athletes to optimize their performance. Boxing consists of many punches, so a series of correct judgments to different types of punches are crucial to competition and training. We design a prototype of smart boxing equipment with the sensor fixed on a boxing pad (Fig. 6a), and the specific experimental configuration is shown in Fig. S13 (Supporting information). Then the boxer wearing PU leather glove punch it using different punches. Following the different types of punches hit on the target point, the analog signals generated by the punches are informative. We choose the most basic punches (jab and uppercut) and an unconventional but distinctive punch (swing) as our samples. Fig. 6b reveals features of the jab, which also called straight punches, and the main technical characteristics of straight punch are as follows. In a fighting stance, the lead fist is launched ahead accompanies with a quick turn of the torso. An overhand punch takes place at the moment of impact. The traits of high initiate speed and the relative longer motion range, as well as rapid recovery action, are all reflected by bi-channel signal. As shown in Fig. 6e<i>, the voltage output amplitude reaches to 28.4 V, which indicate the contact-separation speed is fast. Meanwhile, the contact duration time is 0.05s reflected by the piezoresistive part. Another ubiquitous punch is uppercut (Fig. 6c). It usually initiates from the attacker's belly and thrust upwards in a rising arc before landing on the opponent's face or torso, the fist is thrown at close range. Because of the characteristic of short motion range, it hardly reaches a high contact speed. Meanwhile, the uppercut owns the intention of doing more damage, and it often entails a relatively long contact period. These two traits reflect in electrical signals are the relatively lower amplitude of voltage outputs in the TENG (−7.6V) and long duration time (0.32 s) of pressed state in the Piezoresistance part, respectively, as shown in Fig. 6e<ii>. Another unconventional punch introduced in Fig. 6d is swing. It starts by swing the entire arm through the rotating torso. The impact surface is in the flank of the fist, the area between the index finger and the thumb, but this area the grove is uneven, so it induces the turbulent outputs in the press sensing part. Meanwhile, the lowest amplitude of triboelectric outputs takes place in the inadequate contact situation, as shown in Fig. 6e<iii>. This hybrid sensor distinct three main categories of punches by bi-channel signal criteria. The hybrid sensor can sense the impact with varied motion patterns and has great potential in intelligent sports facilities. Which can feedback not only action effects and boxing sequences in training but also judge scores in the game.

3. Conclusions

In summary, a TENG sensing unit and a piezoresistive sensing unit are unified in a hybrid tactile sensor. The hybrid sensor is mechanically resilient and robust, and the bi-channel signals are easily synchronized to produce a robust judgment. The synergy of the two sensing units enables the sensor to not only measure the pressure but also detect the approaching speed and direction during a mechanical loading process. With the capability to know how much force is applied and how it is applied, the tactile sensor can distinguish different mechanical stimulus, as well as differentiate nuances among similar stimuli. The triboelectric voltage output of the sensor as a function of approaching/separating speed exhibits good linearity up to 100 mm s^{-1}. Hence, the kinematic features of the approaching/separating motion can be partly deduced from the sensor output. We employed the hybrid sensor in a smart boxing pad to identify the different styles of boxing punches. The successful demonstration indicates that this hybrid sensing mechanism has a great potential for smart sport-training, robotic operation, and human-machine interface.

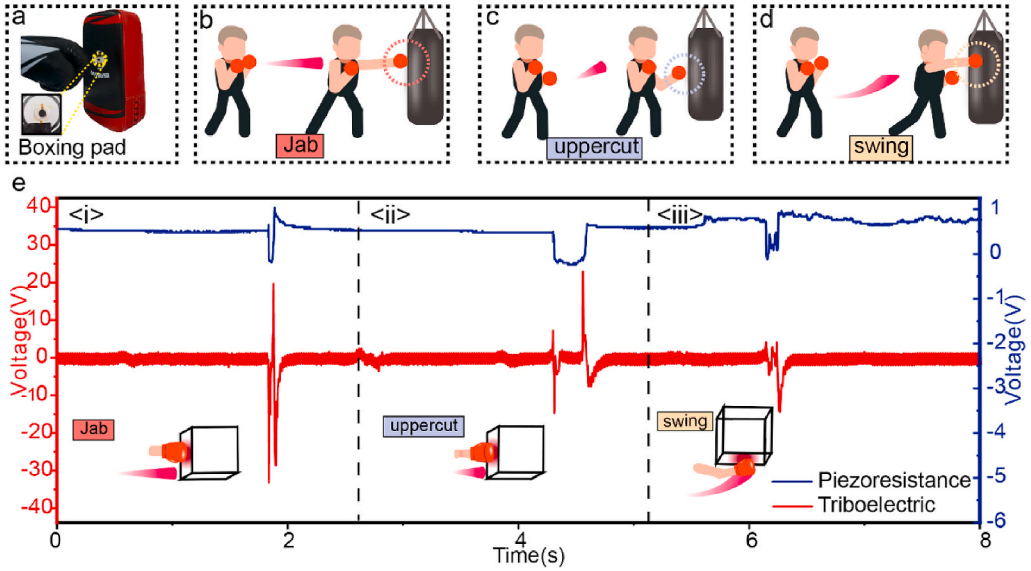

Fig. 6. Application in smart boxing pad. a) Photograph of the boxing pad b-d) Technical characteristic of jab, uppercut, and swing. e) Different bi-channel signals generated by three kinds of punches on the smart boxing pad.

3.1. Experimental methods

Preparation of materials: The mixture prepared for making piezoresistive sensing cell is composed of liquid TPU and filler. TPU particles (Elastollan 35A, BASF) were desiccated in a vacuum drying oven (TAISITE, DZ53T) for 24h and then were dissolved in N, N-dimethylformamide (DMF) solvent in a 1:2 wt ratio (TPU: DMF). After the TPU was completely dissolved, a filler prepared by evenly mixing CB (SUPER P Li, TIMCAL) and NaCl particles (diameter between 300 μm and 355 μm) with a weight ratio of 1:25, then added it into liquid TPU in a weight ratio of 5.2:3. (i.e., the ratio weight of CB: NaCl: TPU is 0.2: 5: 3). The mixture prepared for fabricating the friction layer of TENG made in following way: NaCl particles (diameter between 300 μm and 355 μm) mixed with the base of PDMS (Sylgard 184, Dow Corning) in a weight ratio of 2:1, and add the curing agent of PDMS into the mixture as the weight ratio of base: agent is 1: 20.

Characterization of the device: The mechanical measurements are carried out by a uniaxial tensile and compression testing instruments (Instron, E1000). A digital multimeter (Keysight, 34465A) was employed to measure the resistance variation. Wheatstone bridge was cooperated with DC power supply (KEITHLEY, 2230G-30-3) on converting the resistance variation into voltage change, and it was measured by a digital oscilloscope (ZLG, ZDS2024B Plus) via a 10:1 oscilloscope probe. The output voltage of the TENG was measured via a 100:1 probe. And, its short-circuit current was measured by a low noise current preamplifier (Stanford, SR570). The cross-section morphology of porous conductive TPU and porous PDMS was observed using an SEM (Hitachi, SU8010).

CRediT authorship contribution statement

Zhihao Ma: Methodology, Investigation, Data curation, Writing - original draft, Visualization. **Bo Meng:** Conceptualization, Methodology, Investigation, Writing - original draft. **Ziya Wang:** Methodology. **Chaocheng Yuan:** Investigation. **Zhangwei Liu:** Visualization. **Weiguan Zhang:** Methodology. **Zhengchun Peng:** Conceptualization, Supervision, Writing - review & editing.

Declaration of competing interest

The authors declare that they have no known competing financial interests or personal relationships that could have appeared to influence the work reported in this paper.

Acknowledgments

Zhihao Ma and Bo Meng contributed equally to this work. This work is supported by the Shenzhen Peacock Team Project (KQTD20170810105439418), National Natural Science Foundation of China (Grand Nos. 61904111, 61671308), Natural Science Foundation of Guangdong Province (Grand No. 2020A1515011487) and Shenzhen Science and Technology Program (Grand Nos. JCYJ20190808142609414, JCYJ20170811172639463, JCYJ20170818091233245).

Appendix A. Supplementary data

Supplementary data to this article can be found online at https://doi.org/10.1016/j.nanoen.2020.105216.

References

[1] K. Dong, Z. Wu, J. Deng, A.C. Wang, H. Zou, C. Chen, D. Hu, B. Gu, B. Sun, Z. L. Wang, Adv. Mater. 30 (2018) 1804944.
[2] H. Wu, Z. Su, M. Shi, L. Miao, Y. Song, H. Chen, M. Han, H. Zhang, Adv. Funct. Mater. 28 (2018) 1704641.
[3] T.P. Huynh, H. Haick, Adv. Mater. 30 (2018) 1802337.
[4] M. Ha, S. Lim, H. Ko, J. Mater. Chem. B 6 (2018) 4043.
[5] T. Chen, Q. Shi, M. Zhu, T. He, L. Sun, L. Yang, C. Lee, ACS Nano 12 (2018) 11561.
[6] B. Zhang, Y. Tang, R. Dai, H. Wang, X. Sun, C. Qin, Z. Pan, E. Liang, Y. Mao, Nano Energy 64 (2019) 103953.
[7] S. Lim, D. Son, J. Kim, Y.B. Lee, J.K. Song, S. Choi, D.J. Lee, J.H. Kim, M. Lee, T. Hyeon, Adv. Funct. Mater. 25 (2015) 375.
[8] L.J. Pan, A. Chortos, G.H. Yu, Y.Q. Wang, S. Isaacson, R. Allen, Y. Shi, R. Dauskardt, Z.N. Bao, Nat. Commun. 5 (2014) 3002.
[9] C. Mu, Y. Song, W. Huang, A. Ran, R. Sun, W. Xie, H. Zhang, Adv. Funct. Mater. 28 (2018) 1707503.
[10] Z. Wang, X. Guan, H. Huang, H. Wang, W. Lin, Z. Peng, Adv. Funct. Mater. 24 (2019) 3332.
[11] T. Li, L. Qin, X. Wang, Z. Xiong, H. Ding, Y. Gu, Z. Liu, T. Zhang, Small 12 (2016) 5042.
[12] M. Kang, J. Kim, B. Jang, Y. Chae, J.H. Kim, J.H. Ahn, ACS Nano 11 (2017) 7950.
[13] W.Z. Wu, X.N. Wen, Z.L. Wang, Science 340 (2013) 952.
[14] M.T. Chorsi, E.J. Curry, H.T. Chorsi, R. Das, J. Baroody, P.K. Purohit, H. Ilies, T. D. Nguyen, Adv. Mater. 31 (2019) 1802084.
[15] S. Wang, L. Lin, Z.L. Wang, Nano Energy 11 (2015) 436.
[16] L. Schein, Science 316 (2007) 1572.
[17] L.S. McCarty, G.M. Whitesides, Angew. Chem. Int. Ed. 47 (2008) 2188.
[18] S. Niu, Y. Liu, S. Wang, L. Lin, Y.S. Zhou, Y. Hu, Z.L. Wang, Adv. Funct. Mater. 29 (2014) 1807569.
[19] J. Nie, Z. Ren, L. Xu, S. Lin, F. Zhan, X. Chen, Z.L. Wang, Adv. Mater. 32 (2020) 1905696.
[20] S. Li, Y. Fan, H. Chen, J. Nie, Y. Liang, X. Tao, J. Zhang, X. Chen, E. Fu, Z.L. Wang, Energy Environ. Sci. 13 (2020) 896.
[21] S. Li, J. Nie, Y. Shi, X. Tao, F. Wang, J. Tian, S. Lin, X. Chen, Z.L. Wang, Adv. Mater. 32 (2020) 1905696.
[22] C.A. Mizzi, A.Y. Lin, L.D. Marks, Phys. Rev. Lett. 123 (2019) 116103.
[23] S. Lin, L. Xu, W. Tang, X. Chen, Z.L. Wang, Nano Energy 65 (2019) 103956.
[24] Y. Zi, S. Niu, J. Wang, Z. Wen, W. Tang, Z.L. Wang, Nat. Commun. 6 (2015) 8376.
[25] X.S. Zhang, M.D. Han, R.X. Wang, F.Y. Zhu, Z.H. Li, W. Wang, H.X. Zhang, Nano Lett. 13 (2013) 1168.
[26] L. Cheng, Q. Xu, Y. Zheng, X. Jia, Y. Qin, Nat. Commun. 9 (2018) 3773.
[27] H. Yang, Y. Pang, T. Bu, W. Liu, J. Luo, D. Jiang, C. Zhang, Z.L. Wang, Nat. Commun. 10 (2019) 2309.
[28] W. Tang, T. Jiang, F.R. Fan, A.F. Yu, C. Zhang, X. Cao, Z.L. Wang, Adv. Funct. Mater. 25 (2015) 3718.
[29] F.R. Fan, W. Tang, Z.L. Wang, Adv. Mater. 28 (2016) 4283.
[30] R. Hinchet, H.J. Yoon, H. Ryu, M.K. Kim, E.K. Choi, D.S. Kim, S.-W. Kim, Science 365 (2019) 491.
[31] Q. Zheng, Y. Zou, Y. Zhang, Z. Liu, B. Shi, X. Wang, Y. Jin, H. Ouyang, Z. Li, Z. L. Wang, Sci. Adv. 2 (2016), e1501478.
[32] G. Zhu, C. Pan, W. Guo, C.Y. Chen, Y. Zhou, R. Yu, Z.L. Wang, Nano Lett. 12 (2012) 4960.
[33] X.S. Zhang, M.D. Han, B. Kim, J.F. Bao, J. Brugger, H.X. Zhang, Nano Energy 47 (2018) 410.
[34] H. Chen, Y. Song, M. Han, X. Cheng, H.X. Zhang, Nano Energy 56 (2019) 252.
[35] H. Guo, X. Pu, J. Chen, Y. Meng, M.-H. Yeh, G. Liu, Q. Tang, B. Chen, D. Liu, S. Qi, Sci. Robot. 3 (2018) eaat2516.
[36] Y.S. Zhou, G. Zhu, S. Niu, Y. Liu, P. Bai, Q. Jing, Z.L. Wang, Adv. Mater. 26 (2014) 1719.
[37] G.-H. Lim, S.S. Kwak, N. Kwon, T. Kim, H. Kim, S.M. Kim, S.W. Kim, B. Lim, Nano Energy 42 (2017) 300.
[38] Z.H. Lin, G. Zhu, Y.S. Zhou, Y. Yang, P. Bai, J. Chen, Z.L. Wang, Angew. Chem. Int. Ed. 52 (2013) 5065.
[39] Q. Shen, X. Xie, M. Peng, N. Sun, H. Shao, H. Zheng, Z. Wen, X. Sun, Adv. Funct. Mater. 28 (2018) 1703420.
[40] J. Tao, R. Bao, X. Wang, Y. Peng, J. Li, S. Fu, C. Pan, Z. Li Wang, Adv. Funct. Mater. 29 (2019) 1806379.
[41] L. Lin, Y. Xie, S. Wang, W. Wu, S. Niu, X. Wen, Z.L. Wang, ACS Nano 7 (2013) 8266.
[42] G. Yao, L. Xu, X. Cheng, Y. Li, X. Huang, W. Guo, S. Liu, Z.L. Wang, H. Wu, Adv. Funct. Mater. 29 (2019) 1907312.
[43] Z. Ren, J. Nie, J. Shao, Q. Lai, L. Wang, J. Chen, X. Chen, Z.L. Wang, Adv. Funct. Mater. 28 (2018) 1802989.
[44] Y. Yang, H. Zhang, J. Chen, Q. Jing, Y.S. Zhou, X. Wen, Z.L. Wang, ACS Nano 7 (2013) 7342.
[45] B. Meng, W. Tang, Z.H. Too, X. Zhang, M. Han, W. Liu, H. Zhang, Energy Environ. Sci. 6 (2013) 3235.
[46] T. Li, J. Zou, F. Xing, M. Zhang, X. Cao, N. Wang, Z.L. Wang, ACS Nano 11 (2017) 3950.
[47] X. Wang, H. Zhang, L. Dong, X. Han, W. Du, J. Zhai, C. Pan, Z.L. Wang, Adv. Mater. 28 (2016) 2896.
[48] J. Zou, M. Zhang, J. Huang, J. Bian, Y. Jie, M. Willander, X. Cao, N. Wang, Z. L. Wang, Adv. Energy Mater. 8 (2018) 1702671.
[49] X. Wang, M. Que, M. Chen, X. Han, X. Li, C. Pan, Z.L. Wang, Adv. Mater. 29 (2017) 1605817.
[50] H. Chen, L. Miao, Z. Su, Y. Song, M. Han, X. Chen, X. Cheng, D. Chen, H.X. Zhang, Nano Energy 40 (2017) 65.
[51] H. Wang, Y. Song, H. Guo, J. Wan, L. Miao, C. Xu, Z. Ren, H.X. Zhang, X. Chen, Nano Energy 68 (2020) 104316.

Zhihao Ma received his Bachelor's degree in Optoelectronics from Shandong University in 2015. He is currently a graduate student in Shenzhen University. His main research interests focus on the sensing system and flexible electronics.

Dr. Bo Meng is currently an assistant professor at Shenzhen University. He received his Ph.D. in Microelectronics and Solid-State Electronics from Peking University in 2016. His research interest mainly focuses on micro systems and flexible electronics, especially the applications in energy harvesting and active sensing.

Dr. Ziya Wang is currently an associate research fellow at Shenzhen Institute of Artificial Intelligence and Robotics for Society (AIRS). She received her Ph.D. degree in Physics from University of Science & Technology Beijing in 2016. Her research interests focus on tactile perception in robots and soft robots.

Chaocheng Yuan received his Bachelor's degree in University of Electronic Science and Technology of China, in 2016. He is currently a graduate student in Shenzhen University. His research interest mainly focuses on flexible electronics and tactile sensor.

Zhangwei Liu received his undergraduate degree from Anhui Polytechnic University, China in 2017. He is currently a graduate student in Shenzhen University. His research interests are mainly in triboelectric nanogenerator for energy harvesting and its application in wearable electronics.

Weiguan Zhang received his Ph.D. in electronic engineering from the City University of Hong Kong in 2014. Currently, he is an associate research fellow at Shenzhen University. His research interests include microsensors and flexible electronics.

Dr. Zhengchun Peng received his Ph.D. in Mechanical Egineering (with a focus on MEMS) from Georgia Institute of Technology in 2010. He then joined Intel Corp. as a senior R&D engineer in Technology Manufacturing Group. He is currently a distinguished professor at Shenzhen University. His main research interests include flexible & stretchable electronics, nanosensors, MEMS, and microfluidics.